High-Pressure Chemistry

DOI: 10.1002/anie.201001114

Direct Formation of Mesoporous Coesite Single Crystals from Periodic Mesoporous Silica at Extreme Pressure**

*Paritosh Mohanty, Volkan Ortalan, Nigel D. Browning, Ilke Arslan, Yingwei Fei, and Kai Landskron**

A very fundamental principle in nature is close-packed solid-state structures that minimize the "empty space" between atoms. Accordingly, porous structures form only under special conditions that are able to overcome the tendency of close packing. In most cases porosity is created either by templating strategies or by the use of directional bonding effects.[1,2] The former effect is widely used for the preparation of zeolites and mesoporous oxides, while the latter effect is extensively applied for the preparation of porous metal–organic frameworks.[1,2] Most porous materials are only metastable under ambient conditions.[3] Porous materials exposed to high pressure (>1 GPa) typically undergo facile pore collapse. At extreme pressure (>10 GPa) pore collapse can already occur at room temperature. For example, periodic mesoporous silica MCM-41 undergoes pore collapse at room temperature when the pressure exceeds 12 GPa. At high pressure and elevated temperature the tendency for pore collapse becomes even more pronounced because of the enhanced kinetic activation of the chemical bonds.[4]

Recently, we have reported the formation of stishovite nanocrystals from SBA-16 at 12 GPa and 400 °C.[5] Herein, we report the direct formation of a mesoporous coesite from periodic mesoporous silica SBA-16 at 12 GPa and 300 °C without the aid of a template and within a reaction time of only five minutes. The experiment was carried out in a multi-anvil high-pressure assembly placed into a 1500-ton hydraulic press. The experiment yielded well crystalline coesite according to wide-angle powder X-ray diffraction (WAXS) (Figure 1 a). All reflections could be indexed and refined to lattice constants of $a = 7.157(3)$ Å, $b = 12.371(4)$ Å, $c = 7.181(6)$ Å, and $\beta = 120.28°$, which are typical values for coesite (JCPDS file number: 79-0445). The formation of coesite was further proven by Raman spectroscopy, which shows the typical bands for coesite at wavenumbers of 112, 151, 173, 202, 271, 328, 358, 429, 469, and 521 cm^{-1} (Figure 1 b). These values are

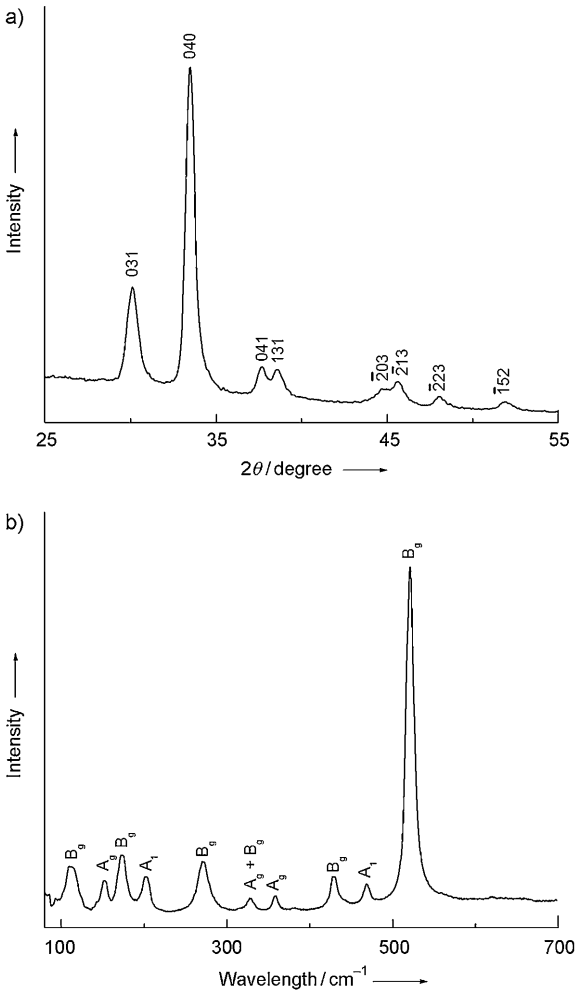

Figure 1. a) Wide-angle X-ray diffraction pattern obtained with $Co_{K\alpha}$ radiation and b) Raman spectrum of mesoporous coesite obtained from SBA-16.

[*] Dr. P. Mohanty, Prof. Dr. K. Landskron
Department of Chemistry, Lehigh University
Bethlehem, PA 18015 (USA)
Fax: (+1) 610-758-6536
E-mail: kal205@lehigh.edu
Homepage: http://www.lehigh.edu/~kal205
Dr. V. Ortalan, Prof. Dr. I. Arslan
Department of Chemical Engineering and Materials Science
University of California at Davis
Davis, CA 95616-5294 (USA)
Prof. N. D. Browning
Department of Chemical Engineering and Materials Science
Department of Molecular and Cellular Biology
University of California at Davis
Davis, CA 95616 (USA)
and
Condensed Matter and Materials Division
Physical and Life Sciences Directorate
Laurence Livermore National Laboratory
Livermore, CA 94550 (USA)
Dr. Y. Fei
Geophysical Laboratory, Carnegie Institution of Washington
Washington, DC, 20015 (USA)

[**] We thank Lehigh University and the Carnegie Institution of Washington for financial support.

Supporting information for this article is available on the WWW under http://dx.doi.org/10.1002/anie.201001114.

in good accordance with literature Raman data for coesite and can be assigned to the B_g, A_g, B_g, A_1, B_g, $A_g + B_g$, A_g, B_g, A_1, and B_g vibrations.[6] According to the phase diagram of silica, stishovite is the expected phase at the respective pressure and temperature conditions. The formation of coesite in the stability field of stishovite indicates that the crystallization is kinetically controlled. The crystallization pathway leads through a coesite intermediate. Owing to the mild crystallization temperature of 300 °C, the coesite phase is stable enough not to convert further into stishovite at a significant rate. The observation of coesite in the stability field of stishovite is in accordance with the Ostwald step rule, which states that a system tends to crystallize first in its least stable polymorph.

To elucidate the morphology of the coesite obtained, we investigated the product by transmission electron microscopy (TEM). To our surprise, the TEM images indicated a highly porous morphology with a mesoscale texture (Figure 2a–c). The images indicated spherically to elliptically shaped pores with diameters between approximately 2 and 50 nm. The pore system does not exhibit periodic order. The pore wall diameters are in the same size regime as the pores. No specific particle shape was observed. To investigate whether the porous particles were crystalline we performed selected area electron diffraction (SAED). The electron diffraction pattern revealed bright regular diffraction spots which indicate that the crystals are magnitudes larger than the mesopores (Figure 2d). The crystals can therefore be described as mesoporous single crystals. The porosity was further studied by scanning electron microscopy (SEM). SEM confirmed the presence of mesoporosity (Figure 3). The images show spherical and elliptical pores and pore walls with diameters of approximately 15–50 nm. The smaller pores (< 15 nm) could not be clearly

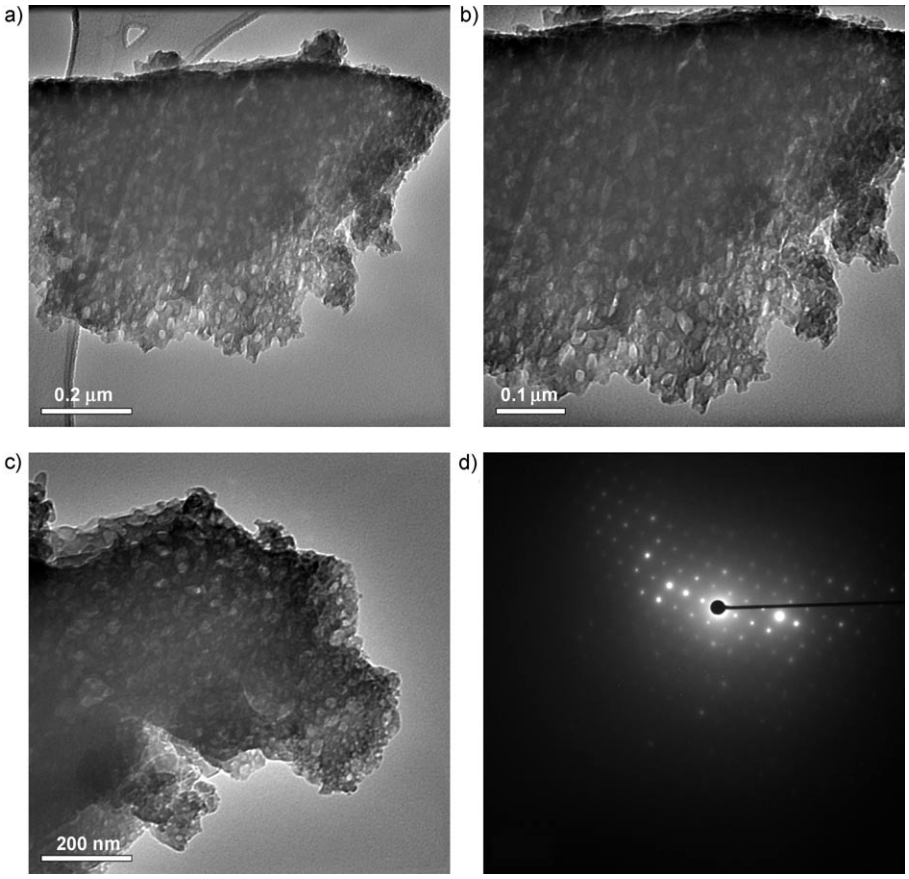

Figure 2. TEM images (a–c) and SAED pattern of mesoporous coesite obtained from SBA-16.

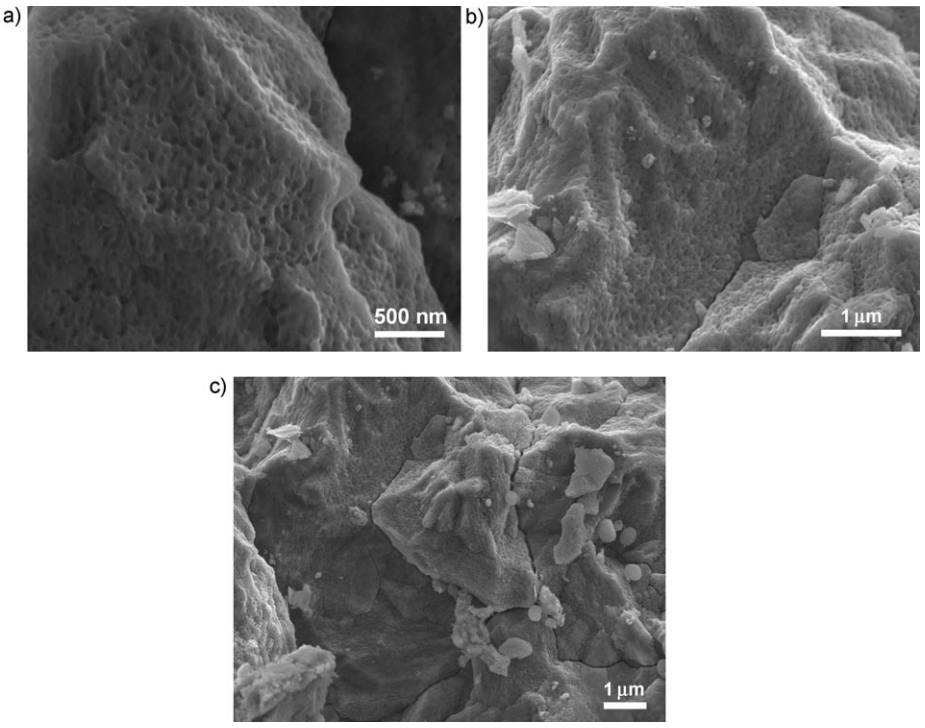

Figure 3. SEM images of mesoporous coesite obtained from SBA-16.

observed in the SEM images due to the lower resolution of the SEM images compared to the images obtained with the TEM technique. Figure 3c shows that the regular mesoporosity extends over a wide area, demonstrating that the sample is homogeneously mesoporous. No appreciable amounts of nonporous particles or nonporous areas within a specific particle were observed.

To confirm the porous nature of the coesite and to obtain more quantitative information about porosity and the pore system we attempted to perform electron tomography. Unfortunately, the specimen is susceptible to beam damage during the measurements and the pores collapsed within seconds. Therefore, a through-focal series of TEM images were collected by aberration corrected electron microscopy that allowed for optically sectioning the specimen at low electron doses.[7] We calculated the total volume of one particular particle to be $14.301 \times 10^{-14}\,cm^3$ and the total volume of the pores within this particle to be $6.994 \times 10^{-14}\,cm^3$. Because of the elongated probe profile in the electron beam direction a correction of these values is required. Including the effect of elongation in the probe the total volume of the probe was calculated to be $6.994 \pm 1.390 \times 10^{-14}\,cm^3$ (Figure 4a). Based on this analysis we found the volume percentage of the pores to be $(49 \pm 9)\,\%$. Likely, the porosity is in the upper range of this value (ca. 55 %) because the lower limit of the porosity assumes that all pores are perfect spheres. The surface area was calculated to be $53\,m^2\,g^{-1}$. The relatively low surface area is plausible considering the single crystallinity of the material which is consistent with low surface roughness. The pore size distribution was calculated by using three different particles for more reliable statistics and was found to be centered around 4 nm, clearly demonstrating that the sample is mesoporous (Figure 4b). A small additional maximum in the histogram was also found for the pore sizes at around 30 nm. This maximum corresponds well to the larger mesopores seen by SEM.

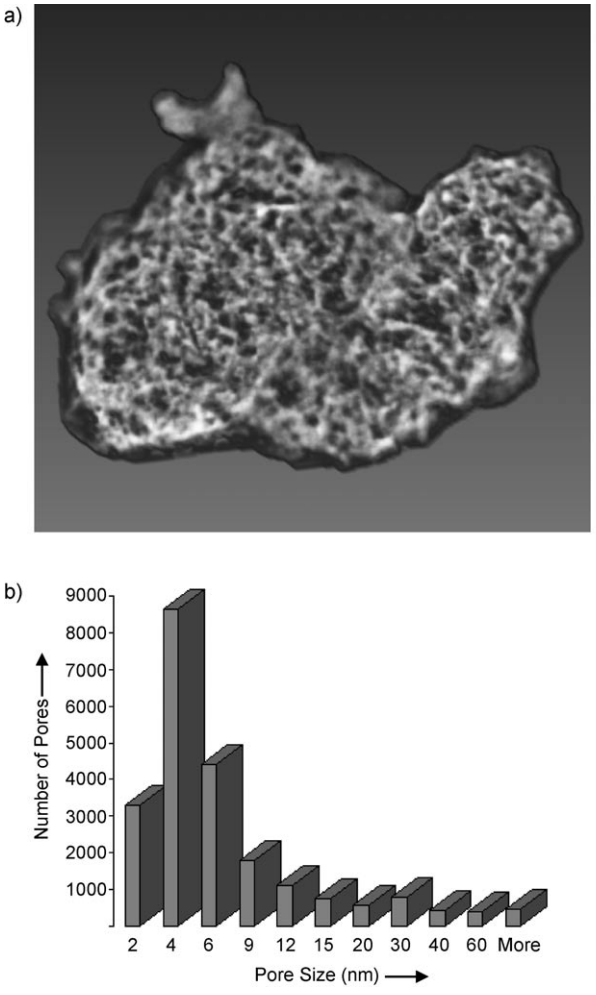

Figure 4. Depth-sectioned electron microscopy (a) and pore size distribution (b) of mesoporous coesite obtained from SBA-16.

A question is: What guides the pore formation at an extreme pressure of 12 GPa? If the observed porosity is a residual porosity of the starting material SBA-16, a mesoporous material should also be obtained at a temperature lower than 300 °C. To clarify this mechanistic question, we conducted an experiment in which we exposed SBA-16 to 200 °C at 12 GPa. The experiment yielded a glassy, almost transparent, monolith which is noncrystalline according to X-ray diffraction (see Figure S1a in the Supporting Information). The entire absence of crystalline coesite was confirmed by Raman spectroscopy (see Figure S1b in the Supporting Information). These findings show that the minimal temperature to crystallize the coesite from SBA-16 lies between 200 and 300 °C, which is a very low crystallization temperature for a SiO_2 material. TEM investigations of the sample recovered from 200 °C did not reveal any mesostructural texture, suggesting that the mesopores are collapsed (see Figure S2 in the Supporting Information). The absence of electronic contrast also confirms that no significant amounts of mesogenic templating species, for example, residual F127 or adsorbed vapors (e.g. adsorbed organic vapors or water) were present during the high-pressure experiment. It is therefore suggested that the mesoporous coesite single crystals form via an intermediate glassy state which is nonporous. The mesoporosity is likely created during the crystallization of the coesite from the nonporous glass. This raises the question: What drives the pore formation during crystallization? Tolbert et al. have shown that the mesopores of MCM-41 can elastically and reversibly deform at high pressure and ambient temperature.[8] Because pore collapse is the ultimate state of pore deformation, it can be assumed that elastic strain exists in the collapsed pore structure of the intermediate glass formed from SBA-16 at 12 GPa. Upon crystallization, the material becomes significantly stiffer and the pores are able to reform. Simultaneously, the crystallization-induced volume shrinkage may further aid the formation of porosity. After the crystallization is complete, the porous coesite remains metastable due to the higher stiffness and inertness of the crystalline coesite channel walls at the mild temperature conditions, and the short reaction times (5 min). The mechanism is shown schematically in Figure 5. This mechanism is supported by the observation of spherical pores that are present in both the SBA-16 as well as the porous coesite material. Moreover, the pore size distribution of the product is centered around 4 nm, which is similar to that of

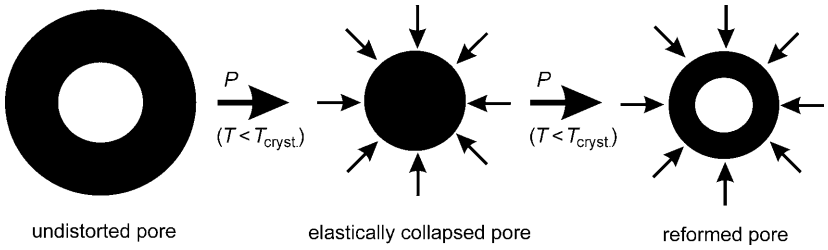

Figure 5. Proposed formation mechanism of mesoporous coesite from periodic mesoporous silicas.

the SBA-16 starting material (5.1 nm). The elastic strain in the glassy intermediate can be clearly seen by polarization microscopy, which shows an anisotropic structure for the glass (see Figure S3 in the Supporting Information). The existence of strain in the glass is further supported by IR spectroscopy (see Figure S4 in the Supporting Information) of the glass and the same glass that has been post-treated at 1000 °C at ambient pressure. The bands for the symmetric (around 800 cm^{-1})[8] and asymmetric Si–O stretching vibrations (around 1100 (transverse vibration)[8] and 1200 cm^{-1} (longitudinal vibration))[8] of the post-treated sample are shifted to higher wavenumbers in comparison to those of the as-synthesized sample, which indicates a decrease of the Si-O-Si intertetrahedral bond angle and a decrease of strain. The as-synthesized material also exhibits an additional band at 950 cm^{-1} that completely disappears upon heating. Density measurements of the glass revealed a density of 2.18 $g\,cm^{-3}$, which is only slightly lower to that of quartz glass (ca. 2.2 $g\,cm^{-3}$).[9] This corroborates that no templating species are present in the glass and that the mesoporous coesite forms from a strained nonporous intermediate glass during crystallization without the aid of a template. A conceivable alternative mechanism would assume the formation of the mesopores upon decompression. However, this appears very unlikely because in this case also the recovered glass formed at 200 °C would be porous.

We were further interested whether the formation of porous coesite is unique to SBA-16 or if it can be observed also from other periodic mesoporous silica materials. To probe this, we have performed high-pressure experiments with KIT-6 at 12 GPa and temperatures of 200 and 300 °C respectively. For the experiment at 300 °C excellent crystallization was achieved and phase-pure coesite was obtained according to WAXS (see Figure S5 in the Supporting Information). TEM investigations revealed that KIT-6 also yields mesoporous particles (see Figure S6a in the Supporting Information). The pore sizes appear somewhat less regular compared to those of the product obtained from SBA-16. Next to large pores with diameters of approximately 20–30 nm there are pores that are about an order of magnitude smaller (around 2–3 nm). SAED showed very bright spots demonstrating that the porous particles are highly crystalline (Figure S6b). The diffraction spots are somewhat less regular compared to the coesite obtained from SBA-16 indicating some degree of polycrystallinity. However, the limited number of diffraction spots indicates that only a few crystallites are present in the selected area. SEM of the sample corroborates the mesoporosity. The pores in the 20–30 nm size regime are visible (see Figure S6c in the Supporting Information). Pores as small as 3 nm are below the resolution of an scanning electron microscope and therefore could not be observed. The experiment performed at 200 °C yielded again an X-ray amorphous glassy product (see Figure S7a in the Supporting Information). Absence of crystalline coesite was further confirmed by Raman spectroscopy (see Figure S7b). Transmission electron microscopy of the product revealed neither mesostructural nor any other nanoscopic texture (see Figure S7c). Furthermore, the polarization microscopy image (see Figure S7d) shows an anisotropic structure for the glass similar to that of the glassy sample obtained from SBA-16 (see Figure S3 in the Supporting Information). This confirms that the observed porosity of the coesite is not a residual porosity of the initial mesostructure. Overall, the analogous behavior of SBA-16 and KIT-6 suggests the mesoporous coesite forms by the same formation mechanism.

In conclusion we have demonstrated that single-crystalline mesoporous high-pressure silica phases (coesite) can form directly from periodic mesoporous silicas without the aid of templates. The direct formation of a highly porous material at extreme pressure is very surprising because nature strongly favors dense over porous structures at high pressure. The phenomenon can be explained by the crystallization of a nonporous glassy silica intermediate that "remembers" the original mesoporosity. The memory effect can be explained by elastic strain in the collapsed intermediate structure and crystallization-induced volume shrinkage. The mesoporous coesite is able to exist in a metastable state at the mild temperature of 300 °C (12 GPa).

Experimental Section

Chemicals: Triblock copolymer $EO_{106}PO_{70}EO_{106}$ Pluronic F127 (BASF), tetraethyl orthosilicate (TEOS, Sigma–Aldrich), hydrochloric acid (EMD Chemicals), butanol (Alfa Aesar). All the chemicals were used as-received without further purification. KIT-6 and SBA-16 were prepared according to literature.[10,11]

Multi-anvil experiment: The experiments were carried out in a multi-anvil assembly with a 1500 t hydraulic press. The samples were encapsulated in Pt capsules of 2.5 mm diameter and 3 mm length. A capsule was placed inside an alumina sleeve, a cylindrical Re heater, and a zirconia sleeve for thermal insulation. This assembly was placed inside a Cr_2O_3-doped MgO octahedron with an edge length of 8 mm and a diameter of 14 mm. The octahedron was placed between eight corner-truncated tungsten carbide cubes with pyrophyllite gaskets. The resulting cubic assembly was placed into the press. In the following, the sample was compressed to the final pressure at a rate of 2 $GPa\,h^{-1}$. After the final pressure was reached, the sample was heated to 200 and 300 °C, respectively, at a heating rate of 100 $K\,min^{-1}$. A sample was kept at the final temperature for 5 min and then quenched. The pressure was released at a rate of 3 $GPa\,h^{-1}$. After normal pressure was reached, the samples were extracted from the Pt capsule.

Characterization of the materials: The formation of the product phase, and the study of its structure and microstructures were carried out by X-ray diffraction (XRD), transmission electron microscopy

(TEM), scanning electron microscopy (SEM), Raman, and Fourier transform infrared (FT-IR) spectroscopy. The TEM images were taken on a JEOL JEM-2000 electron microscope operated at 200 kV. Samples for the TEM analysis were prepared by dispersing the particles in acetone and dropping a small volume of it onto a holey carbon film on a copper grid. SEM images of the specimen were recorded on a Hitachi S-4300 SEM. The XRD patterns were recorded by using a Bruker High-Star diffractometer with a $Co_{K\alpha}$ radiation source and a Rigaku Rapid II diffractometer with $Mo_{K\alpha}$ radiation. The Raman spectrum of the specimen was collected by using a Horiba-Jobin Yvon LabRam-HR spectrometer equipped with a confocal microscope (Olympus BX-30), a 532 nm notch filter, and a single-stage monochromator. The Raman spectrum was collected with 532 nm excitation (20 mW, YAG laser) in the 100–1200 cm^{-1} region. The spectrum was collected at ambient conditions.

Received: February 23, 2010
Published online: May 6, 2010

Keywords: coesite · high-pressure chemistry · mesoporous materials · mesoporous silica · silicon

[1] J. S. Beck et al., *J. Am. Chem. Soc.* **1992**, *114*, 10834 – 10843.
[2] H. K. Chae et al., *Nature* **2004**, *427*, 523 – 527.
[3] S. Corr, D. Shoemaker, E. Toberer, R. Seshadri, *J. Mater. Chem.* **2010**, *20*, 1413 – 1422.
[4] M. Broyer et al., *Langmuir* **2002**, *18*, 5083 – 5091.
[5] P. Mohanty, Y. Fei, K. Landskron, *J. Am. Chem. Soc.* **2009**, *131*, 2764 – 2765.
[6] L. Liu, T. P. Mernagh, W. O. Hibberson, *Phys. Chem. Miner.* **1997**, *24*, 396 – 402.
[7] A. Y. Borisevich, A. R. Lupini, S. J. Pennycook, *Proc. Natl. Acad. Sci. USA* **2006**, *103*, 3044 – 3048.
[8] J. Wu, L. Zhao, E. L. Chronister, S. H. Tolbert, *J. Phys. Chem. B* **2002**, *106*, 5613 – 5621.
[9] *Handbook of Chemistry and Physics*, 66th ed. (Eds.: R. C. Weast, M. J. Astle, W. H. Beyer), CRC, Boca Raton, **1985–86**, p. F-56.
[10] F. Kleitz, S. H. Choi, R. Ryoo, *Chem. Commun.* **2003**, 2136.
[11] D. Zhao, Q. Huo, J. Feng, B. F. Chmelka, G. D. Stucky, *J. Am. Chem. Soc.* **1998**, *120*, 6024 – 6036.

